Ecological Complexity 6 (2009) 240–245

Contents lists available at ScienceDirect

Ecological Complexity

journal homepage: www.elsevier.com/locate/ecocom

Multifractal modeling of soil microtopography with multiple transects data

F. San José Martínez [a,*], J. Caniego [a], A. Guber [b,c], Y. Pachepsky [b], M. Reyes [d]

[a] Technical University of Madrid (UPM), School of Agronomic Engineering, Department of Applied Mathematics, Av. Complutense, 28040 Madrid, Spain
[b] Environmental Microbial Safety Laboratory, USDA-ARS-BA-ANRI-EMSL, Beltsville, MD 20705, USA
[c] University of California, Riverside, CA, USA
[d] Technical University of Madrid (UPM), School of Informatics, Department of Applied Mathematics, 28660 Boadilla del Monte, Spain

ARTICLE INFO

Article history:
Available online 17 June 2009

Keywords:
Soil roughness
Microtopography
Fractals
Multifractal modeling

ABSTRACT

Soil complexity and environmental heterogeneity may be viewed as a consequence of deterministic chaotic dynamics and therefore highly irregular patterns with so-called multifractal behavior should be common. This approach introduces a distinct viewpoint as compared with fractal models for soil surface roughness based on fractional Brownian motion. It suggests that it would be useful to move away from the fractal geometry of sets towards the multifractal description of singular probability measures, as well as going beyond second order statistics. The goal of this study was to investigate the multifractal behavior of soil microtopography measured on transects. On rectangular 200 cm $\times$ 40 cm plots, point elevation values were obtained and soil microtopography was examined as two-dimensional probability measure. A well-defined multifractal behavior similar to multinomial measures was observed in all cases. The multinomial measures were simulated with a multifractal spectrum close to the spectra of the experimental plots to obtain the synthetic multifractals to evaluate the level of uncertainty in the estimates of the multifractal spectrum of natural roughness as a consequence of the transect rather than grid sampling. We found that the transect separation used to collect the experimental data in this work generates a realistic multifractal spectrum but it cannot precisely define its tails that correspond to asymptotic values of the singularity exponents.

1. Introduction

Soil microtopography is affected by a multitude of processes such as detachment and transport of soil particles by surface runoff, infiltration, depression storage, wind erosion, gas exchange, evaporation or heat flux (Huang, 1998). In turn, some of these processes alter microtopography due to erosion and deposition, and changes in soil microrelief are also indicative of the extent of these processes. In agricultural soils, microtopography is altered by tillage, livestock trampling, consolidation, and erosion and deposition from rain and wind. Cycles of freezing/thawing and wetting/drying also change soil surface microrelief.

A substantial effort has been devoted to the quantification and simulation of soil microtopography to enhance the understanding of the soil processes that are affected by soil surface roughness, and the extent to which these processes transform soil microrelief. Statistical indicators were developed to characterize soil roughness at fine scales as early as the late 1950's—see for example Huang (1998) for a more detailed account. These indicators have been perceived as important but not exhaustive (Huang and Bradford, 1990, 1992). For example, they cannot account for some important features of soil surface that should be viewed in the spatial context. Later, geostatistical tools have been applied which consider the elevation of the soil surface as a realization of a stochastic stable process. The soil surface roughness has been treated as the realization of independent random variable with a covariance which depends only on the spatial separation and not on the actual position. Such variables are called second order stationary or weak stationary stochastic processes. The variograms showing the fractal behavior of microtopography and fractional Brownian motion were used to capture soil surface complexity (Huang, 1998) which was parameterized using the fractal dimension and the so-called crossover length even if the part of the variogram corresponding to large lags could not be accurately described with power laws (Huang, 1998).

The scaling properties shown by many geophysical elements can be understood as the by-product of chaotic nonlinear dynamics. In the context of Earth sciences, the complexity and heterogeneity of soil systems widely observed has been recently cast within the framework of the theory of complex systems (Culling, 1988; Phillips, 1993, 1999; Lovejoy and Schertzer, 2007). Using this theory, soil complexity and environmental hetero-

* Corresponding author.
E-mail address: fernando.sanjose@upm.es (F. San José Martínez).

1476-945X/$ – see front matter © 2009 Elsevier B.V. All rights reserved.
doi:10.1016/j.ecocom.2009.05.002

geneity may be viewed as a consequence of the deterministic chaotic dynamics; and highly irregular patterns with so-called multifractal behavior are likely to be found (Beck and Schlögl, 1995; Lovejoy and Schertzer, 1998, 2007). This point of view suggests a move away from the fractal geometry of sets towards the multifractal description of singular probability measures, and also goes beyond second order statistics.

Recently, it has been reported (Gagnon et al., 2006; Lovejoy and Schertzer, 2007) that topography exhibits multifractal behavior over a wide range of scales from 1 to 10^7 m and it has been suggested that this is a consequence of the strong coupling of nonlinear geophysical processes which produce a nonlinear chaotic dynamics. Presumably, we should encounter the same dynamics at finer scales. In this context, the goal of this study was to investigate the multifractal behavior of soil microtopography. For this, point elevation values were examined as a two-dimensional probability measure to determine the presence of multifractal patterns. We also investigate the transect sampling impact on multifractal parameters.

2. Theory

The multifractal analysis of a probability distribution or mass distribution in a rectangular region of the plane requires a set of different grids with rectangular cells. A common choice for the grids is to consider dyadic downscaling (Evertsz and Mandelbrot, 1992; Kravchenko et al., 1999). This may be achieved by successive dyadic partitioning of each side of the rectangular region support of the measure with a factor $\varepsilon = 2^{-k}$ (k = 1, 2, 3,...). At each size scale ε, a number $N(\varepsilon) = 2^{2k}$ of cells are considered and their respective measures $\mu_i(\varepsilon)$ are found from data. Presumably, data should be normalized – i.e. $\sum_{i=1}^{N(\varepsilon)} \mu_i(\varepsilon) = 1$ – in order to have a probability measure.

The number $\alpha_i(\varepsilon) = \log \mu_i(\varepsilon)/\log \varepsilon$ is the *singularity* or *Hölder exponent* of the *i*-th cell of size ε or the *coarse singularity exponent*. We will call it 'singularity exponent' for short. This exponent may be interpreted as a crowding index or a degree of concentration of μ: the greater this value, the smaller the concentration of the measure will be, and vice versa. It is, in fact, the logarithmic density of the *i*-th cell of the partition of characteristic size ε. Typically, coarse singularity exponents of multifractal distributions show a great variability. Moreover, in the limit ($\varepsilon \to 0$ they become a continuum filling up a whole interval $[\alpha_{min}, \alpha_{max}]$. To characterize the different scalings of the measure, the set I_α of points with singularity exponent equal to α is considered and its Hausdorff dimension $\dim_H I_\alpha$ computed. The function $f(\alpha) = \dim_H I_\alpha$ is called the *singularity spectrum* of the distribution μ and quantifies in geometrical and statistical sense the singular behavior of the measure. It gives the "sizes" of the sets where singularity exponents are located and it is related to the probability distribution of these exponents (see Evertsz and Mandelbrot (1992) for details).

Following Chhabra and Jensen (1989), the singularity spectrum may be computed through a set of real numbers q by

$$\alpha(q) \propto \frac{\sum_{i=1}^{N(\varepsilon)} \mu_i(q,\varepsilon) \log \mu_i(\varepsilon)}{\log \varepsilon} \tag{1}$$

and

$$f(\alpha(q)) \propto \frac{\sum_{i=1}^{N(\varepsilon)} \mu_i(q,\varepsilon) \log \mu_i(q,\varepsilon)}{\log \varepsilon} \tag{2}$$

where the quantities $\mu_i(q,\varepsilon)$ are defined by

$$\mu_i(q,\varepsilon) = \frac{\mu_i(\varepsilon)^q}{\sum_{i=1}^{N(\varepsilon)} \mu_i(\varepsilon)^q}. \tag{3}$$

Here the symbol "$\propto$" means scaling or asymptotic behavior as $\varepsilon \to 0$ and the summations run over the cells with nonzero mass (Evertsz and Mandelbrot, 1992).

Expression (3) defines a family of measures parameterized by q. They can be viewed as different distortions of the original measure as parameter q varies. On one side, the larger the parameter q the more heavily large concentrations are weighted, then, for large q's the highest μ_I's dominate the sum. On the other side, the lowest (nonzero) μ_I's yield the dominating contributions for small q's. Finally, we consider the limit measures $\mu(q)$. They are obtained from Expression (3) as the linear size of the partition ε approaches zero. Hence parameter q provides a scanning tool to scrutinize the singularity regions of the measure. For $q \gg 1$, $\mu(q)$ amplifies the regions where μ has a high degree of concentration while, for $q \ll -1$, the regions with a small degree of concentration are magnified. Let us note that $\mu_i(\varepsilon) = \mu_i(1,\varepsilon)$ and the measure μ itself is replicated. When $q = 0$, $\mu_i(0,\varepsilon)$ is just the uniform measure over the set of cells of the partition of characteristic size ε with nonzero mass.

The procedure of Chhabra and Jensen (1989) allows the labeling of the singularity exponents as the parameter q. The exponents become a non-increasing function of q. Large (small) values of the parameter q correspond to high (low) degrees of concentration of the measure. This is a natural result: $\alpha(q)$ is obtained as an average of the singularity exponents with respect to the probability measure $\mu(q)$ that magnifies the denser (more rarefied) regions for large (small) values of q. In particular, $\alpha(0)$ is the average of the singularity exponents weighted by the uniform distribution over the support of μ, so that the sets where the measure is most concentrated are weighted in a similar way to those where it is most rarefied; however, the average is weighted by the probability measure itself in the case of $\alpha(1)$.

This procedure allows also to interpret the fractal dimension $f(\alpha(q))$as the *entropy dimension* of the associated measure $\mu(q)$. In fact, the numerator on the right hand side of Expression (2) is simply the Shannon entropy with respect to a mesh of linear size ε of the measure $\mu(q)$ (Chhabra and Jensen, 1989). So, $f(\alpha(q))$ quantifies the degree of heterogeneity of the distribution $\mu(q)$ by measuring the way its Shannon entropy scales as the linear size of the mesh goes to zero.

Therefore, the singularity spectrum is obtained as a curve parameterized by q. It is the set of points with Cartesian coordinates $(\alpha(q),f(\alpha(q)))$. Comparing Expressions (1) and (2) for $q = 1$ one obtains the equality $f(\alpha(1)) = \alpha(1)$. This parameter is the entropy dimension D_I of the distribution μ. Considering the above reasoning for the case $q = 1$, D_I quantifies the degree of heterogeneity of the distribution μ itself by measuring the way its Shannon entropy scales as the linear size of the mesh shrinks and it may also be considered as the average of logarithmic densities or concentrations of the multifractal distribution weighted by μ. It suggests that D_I may be viewed as the expected value of the different concentrations when the distribution itself is taken into account and it also determines the geometrical size of the set where the "main part" of the distribution concentrates.

One method for generating synthetic multifractal measures is to use the techniques developed by Hutchinson (1981) – see also Peitgen et al. (1992) for a practical approach – based on the notion of iterated function systems. A two-dimensional multifractal distribution on the plane over the unit square can be obtained as follows. Let us consider four weights p_i such that $\sum_{i=1}^{4} p_i = 1$ and let us iterate the process depicted in Fig. 1. When this process is extended to its limit, the resulting mathematical object is a two-dimension multinomial probability measure or mass distribution with four weights that is

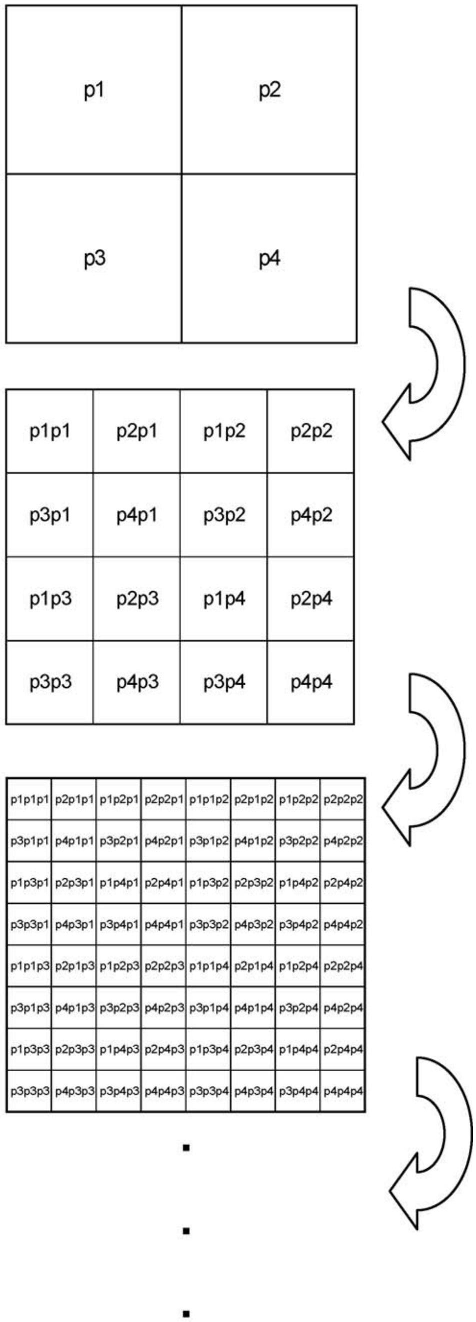

Fig. 1. The iterated process for generating a tetranomial multifractal measure in the unit square of the plate with weights p_i with $i = 1, 2, 3, 4$.

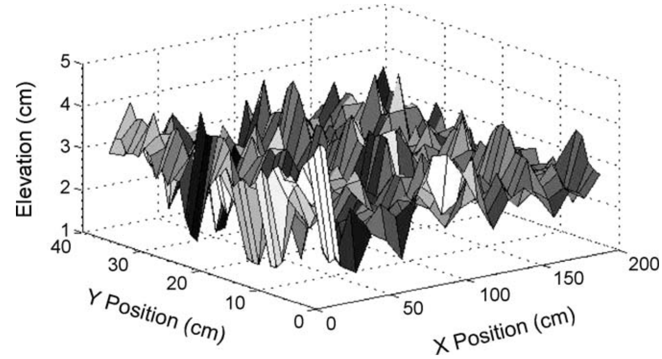

Fig. 2. Graph representing the microrelief of one plot corresponding to the matrix of point elevation values after slope removal.

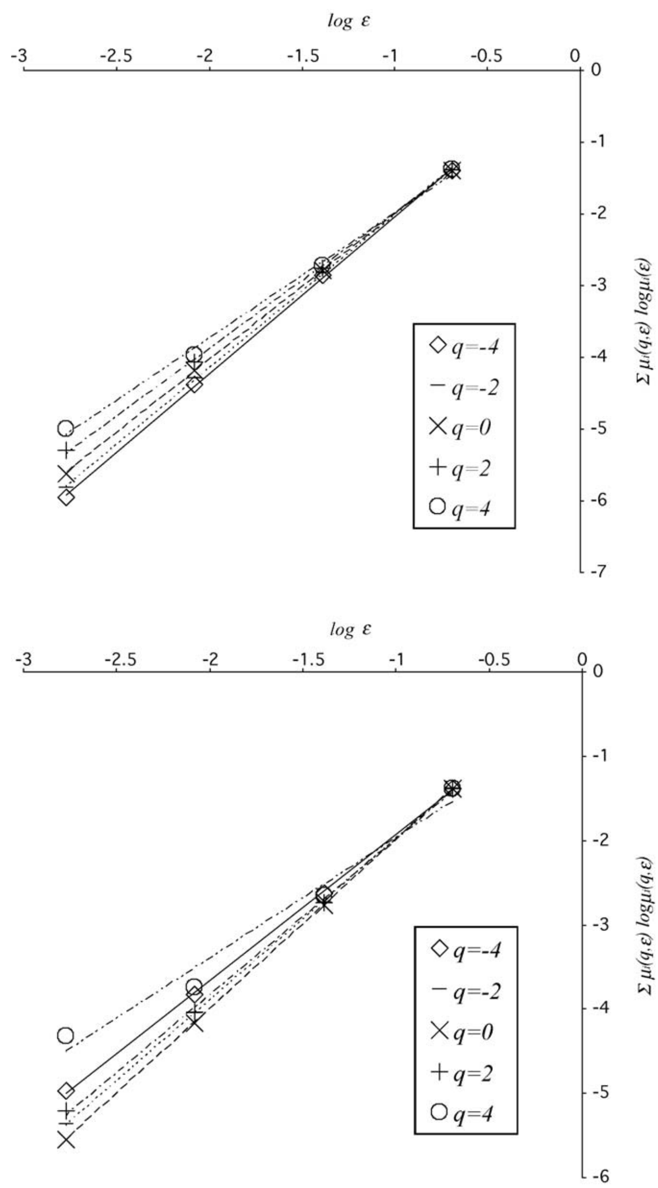

Fig. 3. Scalings of sample A soil microrelief for selected values of parameter q. The graph on the top shows the regression lines to estimate the singularity exponents α and the graph on the bottom the regression lines to estimate the fractal dimensions $f(\alpha)$.

self-similar and multifractal. For obvious reasons we will call these multifractal measures *tetranomials*. It is possible to use close expressions to evaluate their singularity spectrum. Specifically, it can be shown (Evertsz and Mandelbrot, 1992) that

$$\alpha(q) = -\sum_{i=1}^{4}\left(\frac{p_i^q}{\sum_{j=1}^{4} p_j^q}\right)\log_2 p_i \tag{4}$$

and

$$f(\alpha(q)) = -\sum_{i=1}^{4}\left(\frac{p_i^q}{\sum_{j=1}^{4} p_j^q}\right)\log_2\left(\frac{p_i^q}{\sum_{j=1}^{4} p_j^q}\right). \tag{5}$$

These formulae imply that

$$f(\alpha(1)) = \alpha(1) = -\sum_{i=1}^{4} p_i \log_2 p_i, \tag{6}$$

$$\alpha(0) = -\frac{1}{4}\sum_{i=1}^{4} \log_2 p_i, \; f(\alpha(0)) = 2 \tag{7}$$

$$\alpha(-\infty) = \max_i\{-\log_2 p_i\}, \; \alpha(+\infty) = \min_i\{-\log_2 p_i\} \tag{8}$$

Therefore, one way of simulating a multifractal measure with a given multifractal behavior based on its singularity spectrum is to use the above expressions to get a tetranomial multifractal with the same multifractal structure—i.e. both, the original measures and the simulated one should have close multifractal spectra and, as a consequence, values of the above multifractal parameters should also be similar.

3. Materials and methods

Four plots of undisturbed soil under grass were sampled. The plots were 200 cm × 40 cm with a slope of 4% along the longest side. In each plot, 20 transects, 10 cm apart and parallel to the shortest side were considered. The elevation was recorded with 1 cm increment along each transect with the help of a pinmeter (Bryant et al., 2007). The effect of slope of the plots was removed to obtain 4 matrices. They contained 20 columns (transects) and 40 rows (point elevations on each transect) for each plot. Fig. 2 depicts a graph that represents the microrelief of one of these plots.

To study the multifractal behavior of the soil microrelief, point elevation values were normalized and 4 probability measures, one for each plot, were considered. The multifractal parameters were estimated from Expressions (1) and (2) by linear regression using different grids with rectangular cells of sizes which correspond to successive reductions of the rectangular region of the plot by the factors 2^{-k} for $k = 1, 2, 3, 4$. The parameter q was chosen between -4 and 4 in increments of 0.5; hence, we considered 17 possible scalings. Coefficients of determination R^2 of the fit of the linear regression and standard errors *SE* of the estimation of the slope of the regression line were recorded.

4. Results and discussion

The microtopography exhibited a well-defined scaling behavior that represented the fully developed multifractal structure of the soil surface roughness for the plots considered in this study. The coefficients of determination of the fits of the singularity exponents $\alpha(q)$ and the fractal dimensions $f(\alpha(q))$ were all greater than 0.97. Fig. 3 shows the regression lines for the determination of the singularity exponents α and the fractals dimensions $f(\alpha)$ for selected values of parameter q. They correspond to five of the seventeen scalings estimated for sample A. Singularity spectra, depicted in Fig. 4 had a noticeable concave shape with the same pattern: they were asymmetric. This asymmetry was less intense in cases B and D. This particular shape indicates that larger

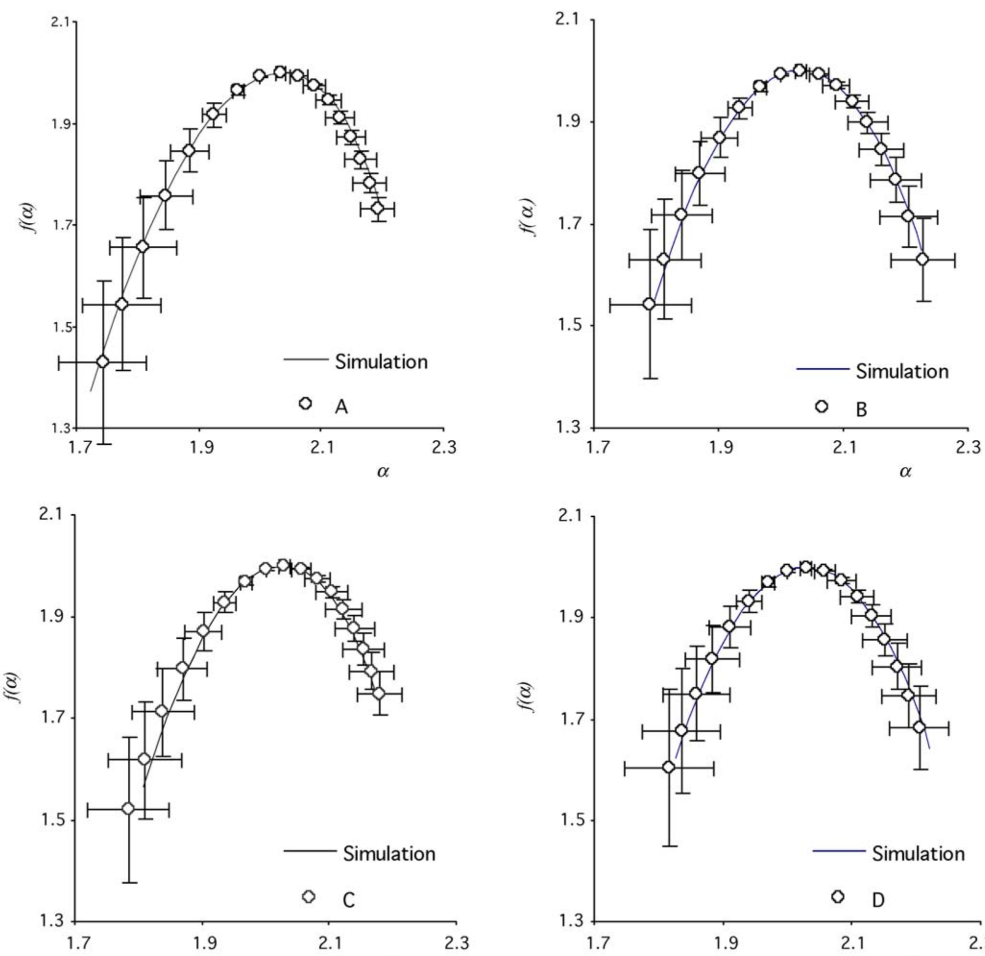

Fig. 4. Singularity spectra of each microrelief with error bars for singularity exponents $\alpha(q)$ and fractal dimensions $f(\alpha(q))$. The estimated values are represented as open circles. Lines represent simulations of two-dimensional tetranomial measures with weights from Table 1.

Table 1
Weights of the simulation of two-dimensional tetranomial measure for each microrelief dataset.

Weights	A	B	C	D
p_1	0.35	0.33	0.33	0.32
p_2	0.23	0.26	0.25	0.27
p_3	0.22	0.22	0.22	0.22
p_4	0.2	0.19	0.2	0.19

concentrations of the measure—i.e. small values of the singularity exponent (Expressions (1) and (2)) corresponding to high point elevation—were more diverse but less common than the smaller concentrations. The left branch was also longer indicating that the geometrical size of the set of points with the smallest exponents α was smaller. At the right branch of the singularity spectrum, we observed the opposite behavior. The highest exponents corresponding to lowest concentrations of the measure were not so diverse but they were more common. In terms of the roughness of the studied soil microrelief, this suggested that the highest peaks were "very" different from one another but that they were "rare" while the lowest depressions were "very" similar to each other and "more frequent". These unbalanced behaviors were less pronounced in datasets B and D which had spectra closer to that of a symmetric concave graph.

The singularity spectra obtained had shapes similar to the spectra of multinomial measures. To support this point we simulated two-dimensional multinomial measures over a unit square with four weights. Iterated functions systems (Hutchinson, 1981; Peitgen et al., 1992) were used to generate self-similar multifractal measures with a grid size corresponding to a dyadic scaling down with a factor of 2^{-9} which corresponds to 9 iterations of the process depicted in Fig. 1. Table 1 shows the weights that were selected for each soil microrelief by adjusting the multifractal parameters estimated from experimental data to the corresponding ones obtained from the tetranomial measures through Expressions (4) and (5). Specifically, we needed to determine four positive numbers, p_1, p_2, p_3 and p_4 which sum equals 1. Let α_{min} and α_{max} are the extreme values estimated for the singularity exponents of a particular experimental measure, then, Expression (8) implies that $\alpha_{min} \approx -\log_2 p_4$ and $\alpha_{max} \approx -\log_2 p_1$, when p_4 is the greatest weight and p_1 is the smallest. Therefore, this provides approximated values for p_1 and p_4. Taking into account that the sum of the four weights is one; only one more condition is needed to determine them. We use Expression (7) to gain an approximated value of $\alpha(0)$; this is the singularity exponent where the maximum of the spectrum is attained. In this way, it was possible to obtain a synthetic soil roughness with a multifractal structure similar to the microtopography of the plots that were studied. Fig. 3 depicts with solid lines the singularity spectra of the tetranomial measures considered for each soil surface microrelief together with experimental spectra and error bars for the singularity exponents α and the fractal dimensions $f(\alpha)$.

To examine the impact of the sampling density on the estimates of multifractal parameters, we used tetranomial measures to carry out a numerical experiment. The synthetic measure was generated by iterating nine times the process depicted in Fig. 1. In this way we obtained a matrix with measures of the cells of a grid with 512×512 cells. This probabilistic measure was viewed as the associated probability measure of a soil microrelief where point elevation values were obtained from points that were 1 cm apart over transects 1 cm apart. This dataset played the role of the full population that was resampled as follows.

Six different squares with 256×256 points were chosen randomly. These were considered to be six random samples of

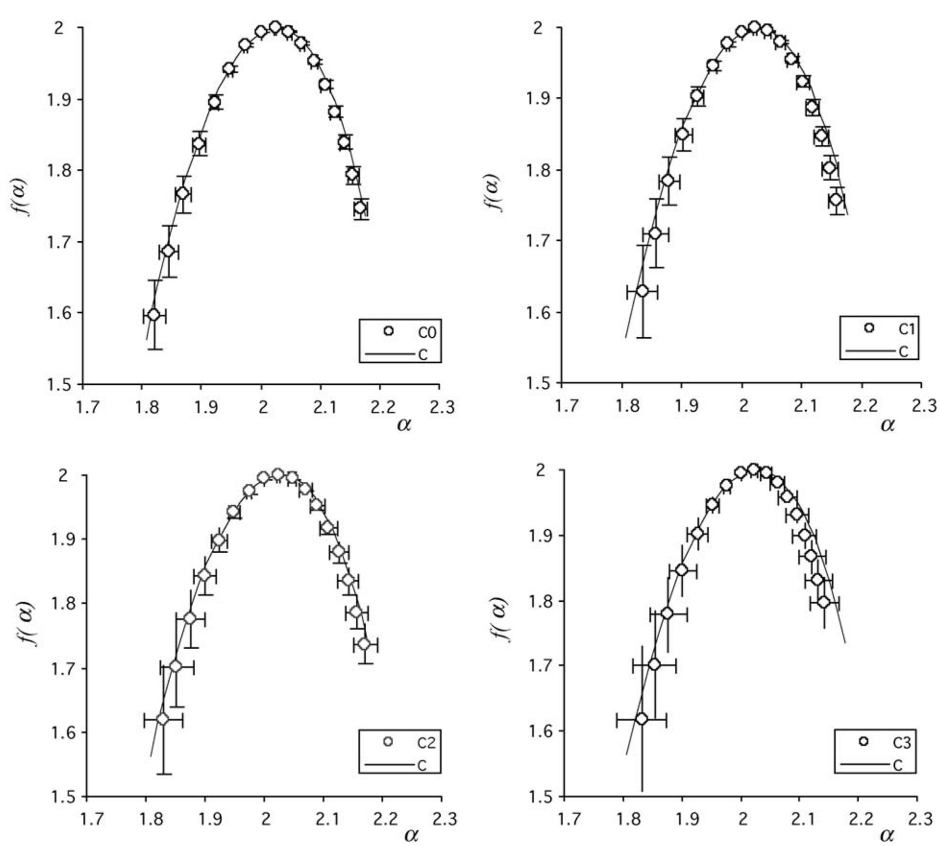

Fig. 5. Multifractal spectra of the sampling of the synthetic tetranomial measure C considering 256 ($C0$), 128 ($C1$), 64 ($C2$) and 32 ($C3$) transects with error bars. Open circles represent the estimated values of the multifractal spectra for the considered sampling densities using Expressions (1) and (2). Lines represent the spectrum of the measure evaluated with Expressions (4) and (5) and weights C from Table 1.

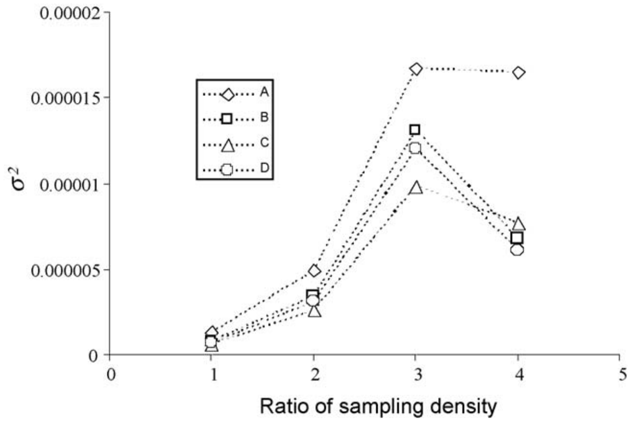

Fig. 6. Variation of the variance with sampling intensity: 256 (1), 128 (2), 64 (4) and 32 (8) transects referred to the ratio of sampling density.

the microtopography. The multifractal spectra of these samples were estimated and compared with the multifractal spectra of the original 512×512 measure obtained by using Expressions (4) and (5). The columns of the 256×256 matrix associated with each sample were considered as transects. Removing columns from each sample, we obtained a series of samples with an increasing distance between transects and less intense sampling. Then we studied four sampling densities. First we removed each second column and obtained a sample with 128 columns. By performing the same operation with this sample, we obtained another one with 64 columns. Then, we obtained six series with four samples, each containing 256, 128, 64 and 32 columns, respectively. Fig. 5 depicts multifractal spectra of one of these series and the spectrum of the original 512×512 measure evaluated with Expressions (4) and (5). Two observations can be made from this. Firstly, the central part of the spectra remained mostly unchanged, and secondly, substantial variations were observed on the tails of the spectra. Therefore, multifractal parameters corresponding to values of parameter q close to zero were robust while those further separated from the center showed more uncertainty. As a consequence, results from the multifractal analysis based on multifractal parameters corresponding to the central part of the spectrum, such as the entropy dimension will be accurate enough with a sampling density similar to the last sample of the series; the one with 32 columns. To obtain the tails of the singularity spectrum, which correspond to extreme values of singularity exponents α or fractal dimensions $f(\alpha)$, the sampling density will be required to be closer to the first sample of the series where transects are 1 cm apart.

We also studied the behavior of the entropy dimension with the sampling density, and we recorded the variance for four sampling densities for the six different 256×256 samples randomly chosen on the original 512×512 measure. As depicted in Fig. 5, the variance of the entropy dimensions grows with the distance between transects and eventually stabilizes. In Fig. 6 the distance between transects was represented as the ratio of the distance between two adjacent transects to the distance of two consecutive sampling points within transects. In this way we got a non-dimensional measure of transects distance or sampling density. These results suggest that the spatial variability of the entropy dimension found from transect measurements is scale-dependent with scale expressed as the distance between transects. Therefore, if one needs to evaluate the significance between the average entropy dimension values found for different surface or vegetation conditions, then, to apply the t-test, the average entropy dimensions and their standard errors have to be, in general, determined at the same scale in terms of the distance between transects. However, if the distances between transects are so large that the scale dependence of the variance does not manifest itself anymore, no scale match in terms of the distances between transects is necessary for statistical comparisons.

5. Conclusions

The roughness of four soil plots microrelief exhibited a well-defined multifractal behavior. Multinomial measures with four weights were generated to simulated soil microrelief. The weights were selected to obtain a good agreement between both, the spectrum of the experimental measure and the spectrum of the tetranomial multifractal. These synthetic multifractals were used to evaluate the uncertainty in the estimates of the multifractal spectrum of natural roughness as a consequence of the distance between two consecutive transects. We found that the distance between transects used to collect the experimental data in this work generates a realistic multifractal spectrum but it cannot define the spectrum tails precisely. At the same time, comparisons of entropy dimensions appear to be possible when the change in the variance with the distance between transects are taken into account. The asymptotic value of the variance can be used in the statistical comparisons of the estimates of the entropy dimensions of roughness obtained in transect sampling if the distance between transects warrants the use of this asymptotic variance value.

Acknowledgments

F.J. Caniego, M. Reyes and F. San José Martínez would like to express their gratitude for the partial support from the Plan Nacional de Investigación Científica, Desarrollo e Innovación Tecnológica (I+D+i) under Reference AGL07-62648, Spain, and UPM (Technical University of Madrid), Reference Q060245024. Special thanks goes to Rocio Torés Barroso for providing assistance to implement numerical computations.

References

Beck, C., Schlögl, F., 1995. Thermodynamics of Chaotic Systems: An Introduction. Cambridge University Press, New York.
Bryant, R., Moran, M.S., Thoma, D.P., Holifield Collins, C.D., Skirvin, S., Rahman, M., Slocum, K., Starks, P., Bosch, D., González, M.P., 2007. Measuring surface roughness height to parameterize radar backscatter models for retrieval of surface soil moisture. IEEE/GRSL 4, 137–141.
Chhabra, A., Jensen, V.J., 1989. Direct determination of the $f(\alpha)$ singularity spectrum. Phys. Rev. Lett. 62, 1327.
Culling, W.E.H., 1988. Dimension and entropy in the soil-covered landscape. Earth Surf. Process. Land. 13, 619–648.
Evertsz, C.J.G., Mandelbrot, B.B., 1992. Multifractal measures. In: Peitgen, H.O., Jürgens, H., Saupe, D. (Eds.), Chaos and Fractals. Springer, Berlin, pp. 921–953.
Gagnon, J.-S., Lovejoy, S., Shertzser, D., 2006. Multifractal earth topography. Nonlin. Process. Geophys. 13, 541.
Huang, C., 1998. Quantification of soil microtopography and surface roughness. In: Baveye, P., Parlange, J.Y., Stewart, B.A. (Eds.), Fractals in Soil Science. CRC Press, 377 pp, pp. 153–168.
Huang, C., Bradford, J.M., 1990. Depressional storage for Markov–Gaussian surfaces. Water Resour. Res. 26, 2235–2242.
Huang, C., Bradford, J.M., 1992. Applications of a laser scanner to quantify soil microtopography. Soil Sci. Soc. Am. J. 56, 14–21.
Hutchinson, J., 1981. Fractals and self-similarity. Indiana Univ. J. Math. 31, 713.
Kravchenko, A.N., Boast, C.W., Bullock, D.G., 1999. Multifractal analysis of soil spatial variability. Agron. J. 91, 1033.
Lovejoy, S., Schertzer, D., 1998. Stochastic chaos and multifractal geophysics. In: Guindani, F., Salvadori, M.G. (Eds.), Fractals and Models 96. Italian University Press, pp. 38–52.
Lovejoy, S., Schertzer, D., 2007. Scaling and multifractal fields in the solid earth and topography. Nonlin. Process. Geophys. 14, 465.
Peitgen, H.O., Jürgen, H., Saupe, D., 1992. Chaos and Fractals: New Frontiers of Sciences. Springer-Verlag, Berlin, pp. 984.
Phillips, J.D., 1993. Stability implications of the state factor model of soils as a nonlinear dynamical system. Geoderma 58, 1–15.
Phillips, J.D., 1999. Earth surface systems: complexity, order and scale. Blackwell, Massachusetts.